SER and Outage Probability Analysis of Double RIS Assisted Wireless Communication System

R. Mahammad Rafi[1] · **V. Sudha[1]**

Abstract

Reconfigurable Intelligent Surface (RIS) can enhance the performance of wireless communication systems in scenarios where there is an obstruction in the direct Line-of-Sight between transceivers. In this paper, we propose a double RIS assisted wireless communication system with no direct link present between source and destination with first RIS (R_1) near to the source, second RIS (R_2) near to the destination, and both RIS will independently assist the communication between source and destination. The analysis includes moment generating function-based symbol error rate evaluation and the derivation of simplified closed-form expression for the outage probability (OP) in terms of the Q-function over Rician and Rayleigh fading channels. A fair comparative performance evaluation, considering an identical number of RIS elements in two systems, is conducted against a single RIS-assisted system with the RIS positioned midway between the source and destination. The analytical findings are corroborated through Monte Carlo simulations and an in-depth examination of the energy consumption gain reveals that the proposed double RIS-assisted system surpasses the single RIS-assisted system in terms of SER and OP while exhibiting lower energy requirements.

1 Introduction

Reconfigurable Intelligent Surface (RIS) play a pivotal role in advancing wireless communication for the next generation [1]. RIS can efficiently manage dynamic wireless environments and provide additional transmission gains, particularly when a direct source-to-destination connection faces obstruction [2]. With the help of passive metamaterial reflective elements, RIS introduces controllable phase shifts to incident electromagnetic

✉ R. Mahammad Rafi
mahammad.rafi402@gmail.com

V. Sudha
vsudha@nitt.edu

1 Department of Electronics and Communication Engineering, National Institute of Technology, Tiruchirappalli, India

waves through a controller connected between the RIS and the source [3]. These intelligent phase shifts constructively enhance the signal-to-noise ratio (SNR) at the desired user, transforming the random wireless channel into a deterministic entity and allowing RIS to create a truly smart radio environment [1, 4].

1.1 Related Works

In the literature, extensive studies on single RIS-aided systems have proven that RIS is a potential energy-efficient technology [5–11]. RIS-assisted single input single output (SISO) system will provide a low bit error rate even in low SNR regimes and outperforms the conventional relay schemes in terms of SER and outage probability [5, 6]. Extensive research has delved into the application of RIS to enhance energy efficiency (EE) across various communication scenarios, including broadcast and multi-user uplink systems [7]. RIS has proven beneficial in supporting ultra-reliable, low-latency scenarios with reduced energy requirements, extended coverage, and minimized latency [8]. Integration with multiple access schemes, such as rate-splitting multiple access and non-orthogonal multiple access (NOMA), has been explored to enhance overall throughput, secrecy and energy efficiency [9–11].

Recent research has highlighted the superior capacity of multi-RIS systems compared to single RIS systems while the configurations with a direct link between source and destination in multi RIS systems show further increase in average achievable rate gains and improved outage probabilities compared to single RIS setups [12–14]. However, practical scenarios may not guarantee such direct links. In [15], the authors have focused on improving outage probability by selecting the RIS with the highest instantaneous SNR among multiple RIS, but the selection strategy of RIS and location of RIS were not covered. Moreover, a multi-RIS aided system will also enhance the physical layer security [16]. However, resource allocation and energy efficiency become significant concerns when using multiple RISs to meet the desired Quality of Service (QoS) [17] and challenges such as reliable channel status information and increased computational complexity with a growing number of RIS were noted [18]. In response to these considerations, a novel double-RIS-assisted system was introduced, placing one RIS near the source and another near the destination [19]. This configuration demonstrated higher beamforming gain and improved wireless communication system secrecy compared to single RIS-assisted systems [20]. However, the double-RIS-assisted system in [19, 20] suffered from high path loss due to double reflection, potentially deteriorating signal power and overall performance. To overcome this issue, we propose a parallel double-RIS system, where two RISs aid communication simultaneously.

Motivated by the above considerations, in this paper, we consider a double RIS-assisted wireless system where two RISs aid communication simultaneously, with R_1 placed near the source and R_2 placed near the destination, without a direct link between the source and destination. The proposed system addresses challenges associated with double reflection, offering promising prospects for practical deployment. For the proposed system, MGF-based SER analysis is developed and a simple expression in terms of Q-function is derived to calculate OP. Additionally, our study considers the dissipated power at the transceivers and RIS circuitry to perform energy consumption gain analysis and showcases the superiority of the proposed double RIS system compared to a baseline single RIS system. All analytical results undergo rigorous verification through Monte Carlo simulations, ensuring the robustness and reliability of our findings.

Table 1 List of symbols and parameters

Symbols and parameters	Description
$\mathbb{E}[X]$	Mean of random variable X
$\mathbb{V}[X]$	Variance of random variable X
$M_\gamma(X)$	Moment generating function of random variable X
t	Non-centrality Parameter of non-central chi-square (NCCS) distribution
v^2	Power in the LoS component
$2\sigma^2$	Power in the non-LoS component
σ_D^2	Noise Power at the destination
$K = v^2/2\sigma^2$	Shape parameter of Rician fading
$L_{1/2}(x)$	Laguerre polynomials of degree 1/2; $L_{1/2}(0) = 1$
$Q_{1/2}(z)$	Generalized Marcum Q-function with fractional order
$Q(z)$	Generalized Marcum Q-function with an integer order
N_1, N_2	Number of reflecting elements in RIS-1, RIS-2
N	Total number of reflecting elements in a single or double RIS system
G_E	Energy consumption gain
P	Transmit power of the source
$P_i, P_c^S and P_c^D$	Dissipated circuit powers at ith RIS element, source, and destination
λ	Operating Wavelength
α	Path loss at a reference distance of 1 m
ϱ	Path-loss exponent

The next section introduces the system model under consideration. Section 3 presents the analysis of SER and the outage probability of the proposed system. Section 4 provides theoretical and simulation results. Finally, Sect. 5 concludes the paper. The list of symbols and parameters used in the paper are given in Table 1.

2 System Model

As shown in Fig. 1, we consider a double-RIS-assisted system consisting of a single antenna source (S) that communicates with a single antenna destination (D), with the assistance of R_1 and R_2. The number of reflecting elements in R_1 and R_2 are N_1 and N_2 respectively. The reflecting elements of each RIS are programmable with the help of RIS controller and it communicates with the source through a separate backhaul link to coordinate transmission and information exchange, such as channel state information and RIS phase shifts. The direct link between source and destination is blocked due to obstacles. The source and destination are in the far field of R_1 and R_2 [8]. It is assumed that the fading channel is quasi-static and flat, with no interference [1]. Further, we assume that the cascaded links from source to destination via each RIS are independent.

Then, the received signal at the destination via two independent paths (S-R_1-D and S-R_2-D) is expressed as follows:
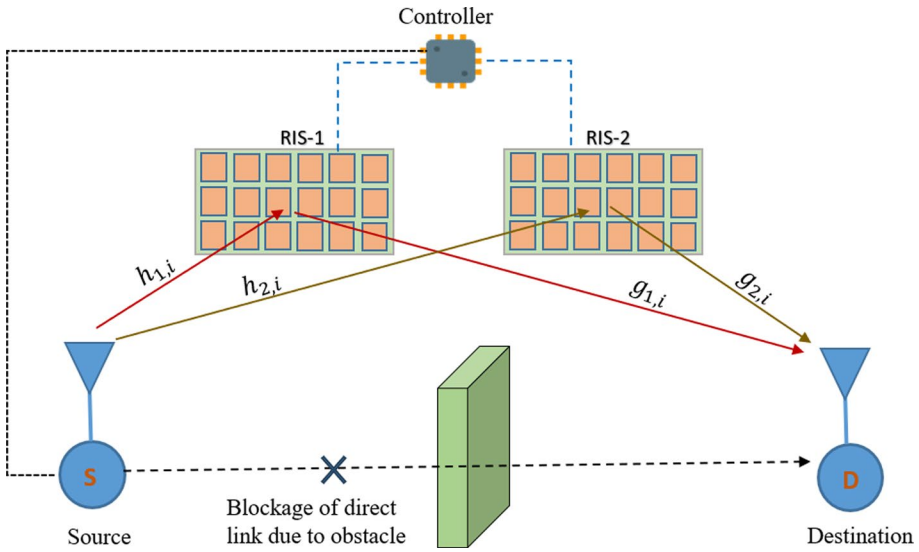
Fig. 1 Proposed Double RIS-assisted wireless communication system

$$y = \sqrt{P}\left[\sum_{i=1}^{N_1} h_{1,i}e^{j\phi_{1,i}}g_{1,i} + \sum_{k=1}^{N_2} h_{2,k}e^{j\phi_{2,k}}g_{2,k}\right]x + n. \tag{1}$$

For simplicity, we assume that each RIS have the same number of elements, i.e., $N_1 = N_2 = N_d$, then Eq. (1) modified as:

$$y = \sqrt{P}\left[\sum_{i=1}^{N_d} h_{1,i}e^{j\phi_{1,i}}g_{1,i} + \sum_{i=1}^{N_d} h_{2,i}e^{j\phi_{2,i}}g_{2,i}\right] + n. \tag{2}$$

In Eq. (2), $\phi_{1,i}$ and $\phi_{2,i}$ are the phase shift introduced by the i th element of RIS-1(R_1) and RIS-2(R_2) respectively; P is the transmit power of the source, x denotes the transmitted signal and $n \sim CN(0, \sigma_D^2)$ stands for additive white Gaussian noise. The channels from S to the i th element of R_1 and i th element of R_1 to D are $h_{1,i} = d_{SR_{1,i}}^{-\varrho/2}\alpha_{1,i}e^{-j\theta_{1,i}}$ and $g_{1,i} = d_{R_{1,i}D}^{-\varrho/2}\beta_{1,i}e^{-j\psi_{1,i}}$ respectively. Similarly, $h_{2,i} = d_{SR_{2,i}}^{-\varrho/2}\alpha_{2,i}e^{-j\theta_{2,i}}$ and $g_{2,i} = d_{R_{2,i}D}^{-\varrho/2}\beta_{2,i}e^{-j\psi_{2,i}}$ are the channels from S to i th element of R_2 and i th element of R_2 to D respectively. Here $\alpha_{1,i}, \alpha_{2,i}, \beta_{1,i}$ and $\beta_{2,i}$ denotes the amplitudes of channel coefficients and $\theta_{1,i}, \theta_{2,i}, \psi_{1,i}$ and $\psi_{2,i}$ denotes the phase of the corresponding channel, and denotes the path loss coefficient. The distances from S to the i element of R_1 and R_2 are denoted as $d_{SR_{1,i}}$ and $d_{SR_{2,i}}$ respectively. Similarly, the distances from i th element of R_1 and R_2 to D are denoted as $d_{R_{1,i}D}$ and $d_{R_{2,i}D}$ respectively. Then the Eq. (2) can be written as,

$$\gamma = \frac{P\left|\sum_{i=1}^{N_d} d_{SR_{1,i}}^{-\varrho/2}\alpha_{1,i}d_{R_{1,i}D}^{-\varrho/2}\beta_{1,i}e^{j(\phi_{1,i}-\theta_{1,i}-\psi_{1,i})} + \sum_{i=1}^{N_d} d_{SR_{2,i}}^{-\varrho/2}\alpha_{2,i}d_{R_{2,i}D}^{-\varrho/2}\beta_{2,i}e^{j(\phi_{2,i}-\theta_{2,i}-\psi_{2,i})}\right|^2}{\sigma_D^2} \tag{3}$$

Under the far-field assumption we can write $d_{SR_{1,i}} = d_{SR_1}$, $d_{SR_{2,i}} = d_{SR_2}$, $d_{R_{1,i}D} = d_{R_1D}$ and $d_{R_{2,i}D} = d_{R_2D}$. Moreover, in the proposed system, R_1 and R_2 are deployed symmetrically such that $d_{SR_1} = d_{R_2D}$ and $d_{SR_2} = d_{R_1D}$, then we have $d_{SR_1}d_{R_1D} = d_{SR_2}d_{R_2D} = d_t$. By assuming that the perfect knowledge of CSI at each RIS [13], i.e., $\phi_{1,i} = \theta_{1,i} + \psi_{1,i}$ and $\phi_{2,i} = \theta_{2,i} + \psi_{2,i}$ then Eq. (3) is modified as Eq. (4).

$$\gamma = \frac{P\left(\sum_{i=1}^{N_d} \alpha_{1,i}\beta_{1,i} + \sum_{i=1}^{N_d} \alpha_{2,i}\beta_{2,i}\right)^2}{\sigma_D^2 d_{tol}^o} = (A+B)^2\overline{\gamma} = C^2\overline{\gamma}. \tag{4}$$

Here , $C = A + B$, $A = \sum_{i=1}^{N} \alpha_{1,i}\beta_{1,i}$, $B = \sum_{i=1}^{N} \alpha_{2,i}\beta_{2,i}$ and $\overline{\gamma} = \frac{P}{\sigma_D^2 d_{tol}^o}$ stands for average SNR.

3 Performance Analysis

This section focuses on deriving mathematical expressions for the symbol error rate (SER) and outage probability (OP) of the proposed system. The analysis considers independent and identical fading for each communication channel. It begins with assumption of a Rician[1] distribution for all communication links, and subsequently adjusts the derived expressions to accommodate the Rayleigh[2] fading scenario.

3.1 SER analysis

In preparation for the analysis of SER of the proposed system, it is essential to compute the statistical parameters of received SNR for Rician and Rayleigh fading scenarios. In Eq. (4), $\alpha_{1,i}$ and $\beta_{1,i}$ follows Rician distribution with mean and variance given by $E[a_{(1,i)}] = E[(\beta)_{(1,i)} = v(p/2)s(L)_{(1/2)}(-v^2/(2s^2))$ and $V[a_{(1,i)}] = V\left[(\beta)_{(1,i)}^2\right] = v^2 + 2s^2 - p/2s^2(L_{(1/2)}(-v^2/(2s^2)))$

Where $K = \frac{Power\, in\, line\, of\, sight\, (LoS)\, component}{Power\, in\, non-LoS(NLoS)component} = \frac{v^2}{2\sigma^2}$ denotes the shape parameter and the statistical parameters of product of $\alpha_{1,i}, \beta_{1,i}$ and all other random variables are obtained in Table 2.

The mean and variance of the product of independent and identical distributed Rican random variables $\alpha_{1,i}$, $\beta_{1,i}$ and $\alpha_{2,i}$, $\beta_{2,i}$ follows Rician distribution with statistical properties as shown in Table 2. With the assumption of $N_d \gg 1$, A, B follows Gaussian distribution as per central limit theorem and $C = A + B$, also follows Gaussian with statistical mean and variance as shown in Table 2. Then γ, the square Gaussian random variable C, follows a non-central chi-square distribution with one degree of freedom (*DoF*) [21] and the MGF of γ is given as [22],

---

[1] Rician fading will be suitable for the scenarios with strong LoS Path such as indoor area.
[2] Rayleigh fading will be suitable for the scenarios with no LoS Path and non-LoS paths such as outdoor environment.

Table 2 The derivation of statistical Parameters of random variables A, B and C

Statistical parameter	Rician	Rayleigh i.e., $K = 0$
$\mathbb{E}[\alpha_{1,i}] = \mathbb{E}[\beta_{1,i}] = \mathbb{E}[\alpha_{2,i}] = \mathbb{E}[\beta_{2,i}]^a$	$\sqrt{\frac{\pi}{2}}\sigma L_{1/2}\left(-\frac{v^2}{2\sigma^2}\right)$	$\frac{\sqrt{\pi}}{2}$
$\mathbb{V}[\alpha_{1,i}] = \mathbb{V}[\beta_{1,i}] = \mathbb{V}[\alpha_{2,i}] = \mathbb{V}[\beta_{2,i}]$	$v^2 + 2\sigma^2 - \frac{\pi}{2}\sigma^2\left(L_{1/2}\left(-\frac{v^2}{2\sigma^2}\right)\right)^2$	$1 - \frac{\pi}{4}$
$\mathbb{E}[\alpha_{1,i}\beta_{1,i}] = \mathbb{E}[\alpha_{2,i}\beta_{2,i}]$	$\frac{\pi}{2}\sigma^2\left(L_{1/2}\left(-\frac{v^2}{2\sigma^2}\right)\right)^2$	$\frac{\pi}{4}$
$\mathbb{V}[\alpha_{1,i}\ \beta_{1,i}] = \mathbb{V}[\alpha_{2,i}\ \beta_{2,i}]^b$	$2\sigma^2 - \frac{\pi^2}{4}\sigma^4\left(L_{1/2}\left(-\frac{v^2}{2\sigma^2}\right)\right)^4 + v^2$	$1 - \frac{\pi^2}{16}$
$\mathbb{E}[A] = \mathbb{E}[B]$	$\frac{N_d\pi}{2}\sigma^2\left(L_{1/2}\left(-\frac{v^2}{2\sigma^2}\right)\right)^2$	$\frac{N_d\pi}{4}$
$\mathbb{V}[A] = \mathbb{V}[B]$	$N_d\left[2\sigma^2 - \frac{\pi^2}{4}\sigma^4\left(L_{1/2}\left(-\frac{v^2}{2\sigma^2}\right)\right)^4\right] + N_d v^2$	$N_d\left(1 - \frac{\pi^2}{16}\right)$
$\mathbb{E}[C] = \mathbb{E}[A] + \mathbb{E}[B]$	$N_d\pi\sigma^2\left(L_{1/2}\left(-\frac{v^2}{2\sigma^2}\right)\right)^2$	$\frac{N_d\pi}{2}$
$\mathbb{V}[C] = \mathbb{V}[A] + \mathbb{V}[B]$	$2N_d\left[2\sigma^2 - \frac{\pi^2}{4}\sigma^4\left(L_{1/2}\left(-\frac{v^2}{2\sigma^2}\right)\right)^4\right] + 2N_d v^2$	$2N_d\left(1 - \frac{\pi^2}{16}\right)$

[a]We assume all the channels are follows the same distribution with identical statistical parameters.
[b]If X and Y are independent random variables, then $\mathbb{E}[XY] = \mathbb{E}[X]\mathbb{E}[Y]$ and $\mathbb{V}[XY] = \mathbb{E}[X]^2\mathbb{V}[Y] + \mathbb{E}[Y]^2\mathbb{V}[X] + \mathbb{V}[X]\mathbb{V}[Y]$

$$M_\gamma(s) = \left(\frac{1}{1 - 2s\mathbb{V}[C]\overline{\gamma}}\right)^{\frac{DoF}{2}} \times exp\left(\frac{st^2}{1 - 2s\mathbb{V}[C]\overline{\gamma}}\right), \tag{5}$$

In Eq. (5), $t = \sqrt{\mathbb{E}[C]^2} = N_d\pi\sigma^2\left(L_{1/2}\left(-\frac{v^2}{2\sigma^2}\right)\right)^2$ denotes the non-centrality parameter of the *NCCS*. Now the MGF of received SNR for the proposed system is written as,

$$M_\gamma(s) = \left(\frac{1}{1 - s\left(N_d v^2 + 8N_d\sigma^2 - N_d\pi^2\sigma^4\left(L_{1/2}\left(-\frac{v^2}{2\sigma^2}\right)\right)^4\right)\overline{\gamma}}\right)^{\frac{1}{2}}$$
$$\times exp\left(\frac{sN_d^2\pi^2\sigma^4\left(L_{1/2}\left(-\frac{v^2}{2\sigma^2}\right)\right)^4\overline{\gamma}}{1 - s\left(N_d v^2 + 8N_d\sigma^2 - N_d\pi^2\sigma^4\left(L_{1/2}\left(-\frac{v^2}{2\sigma^2}\right)\right)^4\right)\overline{\gamma}}\right) \tag{6}$$

From (5), the average SER of *M*-ary phase shift keying (MPSK) signaling is calculated as [22]:

$$P_e = \frac{1}{\pi}\int_0^{(M-1)\pi/M} M_\gamma\left(\frac{-\sin^2(\pi/M)}{\sin^2\eta}\right)d\eta \tag{7}$$

By substituting Eq. (6) in Eq. (7) the closed form expression for the for average SER of MPSK can be given as

$$P_e = \frac{1}{\pi} \int_0^{(M-1)\pi/M} \left(\frac{1}{1 + \frac{\sin^2(\pi/M)\left(N_d v^2 + 8N_d \sigma^2 - N_d \pi^2 \sigma^4 \left(L_{1/2}\left(-\frac{v^2}{2\sigma^2}\right)\right)^4\right)\bar{\gamma}}{\sin^2 \eta}} \right)^{\frac{1}{2}}$$

$$\times exp\left(\frac{\frac{-\sin^2(\pi/M)N_d^{\,2}\pi^2 \sigma^4 \left(L_{1/2}\left(-\frac{v^2}{2\sigma^2}\right)\right)^4 \bar{\gamma}}{\sin^2 \eta}}{1 + \frac{\sin^2(\pi/M)\left(N_d v^2 + 8N_d \sigma^2 - N_d \pi^2 \sigma^4 \left(L_{1/2}\left(-\frac{v^2}{2\sigma^2}\right)\right)^4\right)\bar{\gamma}}{\sin^2 \eta}} \right) d\eta. \tag{8}$$

By substituting $\eta = (M-1)\pi/M$ in Eq. (8), we will get the upper bound of P_e as follows:

$$P_e \leq \frac{(M-1)}{M} \left(\frac{1}{1 + \frac{\sin^2(\pi/M)N_s \Omega^{\frac{4}{\beta}}\left((\Gamma(1+2/\beta))^2 - \Gamma((1+1/\beta))^4\right)\bar{\gamma}}{\sin^2((M-1)\pi/M)}} \right)^{\frac{1}{2}}$$

$$\times exp\left(\frac{\frac{-\sin^2(\pi/M)N_d^{\,2}\pi^2 \sigma^4 \left(L_{1/2}\left(-\frac{v^2}{2\sigma^2}\right)\right)^4 \bar{\gamma}}{\sin^2((M-1)\pi/M)}}{1 + \frac{\sin^2(\pi/M)\left(N_d v^2 + 8N_d \sigma^2 - N_d \pi^2 \sigma^2 \left(L_{1/2}\left(-\frac{v^2}{2\sigma^2}\right)\right)^4\right)\bar{\gamma}}{\sin^2((M-1)\pi/M)}} \right), \tag{9}$$

for binary PSK (BPSK), i.e. for $M = 2$, Eq. (8) and Eq. (9) are simplified to Eq. (10) and Eq. (11) which will give expressions to evaluate the average SER and upper bound of SER respectively.

$$P_e = \frac{1}{\pi} \int_0^{\pi/2} \left(\frac{1}{1 + \frac{\left(N_d v^2 + 8N_d \sigma^2 - N_d \pi^2 \sigma^4 \left(L_{1/2}\left(-\frac{v^2}{2\sigma^2}\right)\right)^4\right)\bar{\gamma}}{\sin^2 \eta}} \right)^{\frac{1}{2}}$$

$$\times exp\left(\frac{\frac{-N_d^{\,2}\pi^2 \sigma^4 \left(L_{1/2}\left(-\frac{v^2}{2\sigma^2}\right)\right)^4 \bar{\gamma}}{\sin^2 \eta}}{1 + \frac{\left(N_d v^2 + 8N_d \sigma^2 - N_d \pi^2 \sigma^4 \left(L_{1/2}\left(-\frac{v^2}{2\sigma^2}\right)\right)^4\right)\bar{\gamma}}{\sin^2 \eta}} \right) d\eta, \tag{10}$$

By substituting $\eta = 1/2$ in Eq. (10), we will get the upper bound of P_e for BPSK signaling scheme as follows:
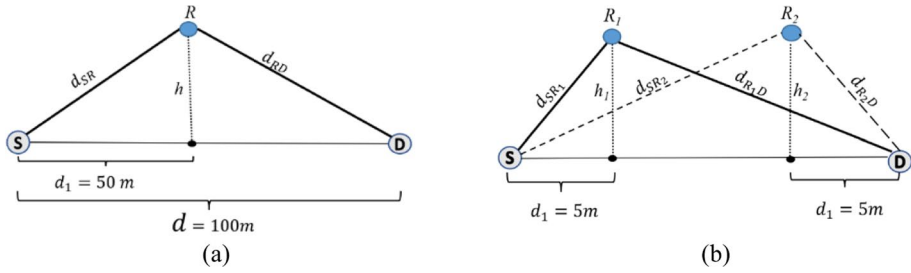
Fig. 2 Simulation Setup: **a** Single RIS **b** Double RIS

$$
P_e \leq \frac{1}{2} \left(\frac{1}{1 + \left(N_d v^2 + 8N_d \sigma^2 - N_d \pi^2 \sigma^4 \left(L_{1/2}\left(-\frac{v^2}{2\sigma^2}\right)\right)^4 \right)\overline{\gamma}} \right)^{\frac{1}{2}}
$$

$$
\times \exp \left(\frac{-N_d^2 \pi^2 \sigma^4 \left(L_{1/2}\left(-\frac{v^2}{2\sigma^2}\right)\right)^4 \overline{\gamma}}{1 + \left(N_d v^2 + 8N_d \sigma^2 - N_d \pi^2 \sigma^2 \left(L_{1/2}\left(-\frac{v^2}{2\sigma^2}\right)\right)^4 \right)\overline{\gamma}} \right).
\tag{11}
$$

For the Rayleigh fading scenario one can get the expressions for SER by simply substituting $v^2 = 0$, $\sigma^2 = \frac{1}{2}$ in Eq. (7). For an instance the expression to evaluate average SER of M-ary phase shift keying (PSK) signaling is given as,

$$
P_e = \frac{1}{\pi} \int_0^{(M-1)\pi/M} \left(\frac{1}{1 + \frac{\sin^2(\pi/M)N_d(16-\pi^2)\overline{\gamma}}{4\sin^2\eta}} \right)^{\frac{1}{2}} exp \left(\frac{-\frac{\sin^2(\pi/M)N_d^2\pi^2\overline{\gamma}}{4\sin^2\eta}}{1 + \frac{\sin^2(\pi/M)N_d(16-\pi^2)\overline{\gamma}}{4\sin^2\eta}} \right) d\eta
\tag{12}
$$

3.2 Outage Probability Analysis:

The probability that the received SNR is less than a specified threshold γ_{th} is known as outage. As we mentioned, in previous section, γ follows a *NCCS* distribution and hence outage probability can be expressed as [15]:

$$
P_{out} = \Pr(\gamma < \gamma_{th}) = 1 - Q_{\frac{1}{2}}\left(\sqrt{\frac{t^2}{\mathbb{V}[C]}}, \sqrt{\frac{\gamma_{th}}{\overline{\gamma}\mathbb{V}[C]}} \right)
\tag{13}
$$

The closed form expression for the outage probability for a threshold γ_{th} in terms of Q-function[3] with integer order of 1 is given as [27],

---

[3] MATLAB lacks direct support for special functions with fractional orders like the Marcum Q function.

Fig. 3 Bit error rate of single RIS and proposed double RIS system versus P for varying N and $K = 0$ assuming BPSK
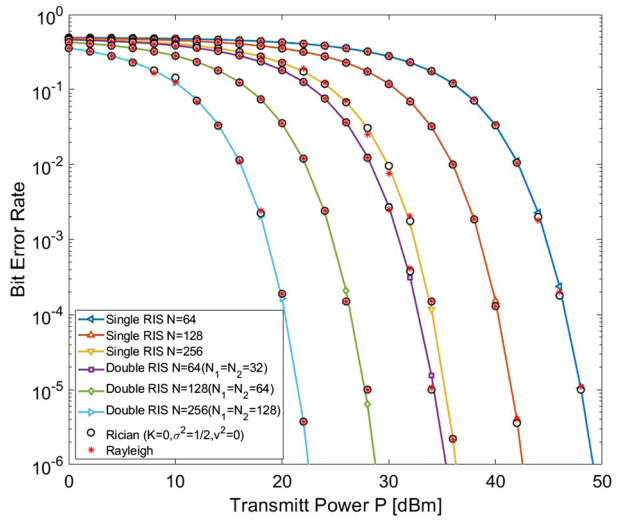
Fig. 4 BER performance of proposed double RIS systems versus P with varying K assuming BPSK
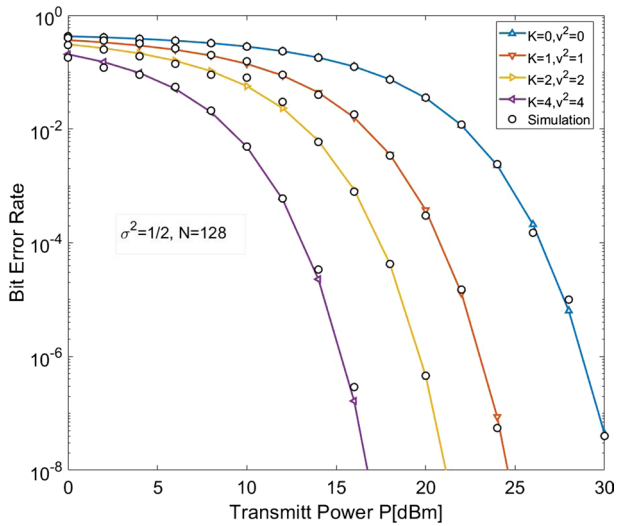
$$P_{out} = 1 - \left(Q\left(\sqrt{\frac{\gamma_{th}}{\bar{\gamma}\mathbb{V}[C]}} - \sqrt{\frac{t^2}{\mathbb{V}[C]}} \right) + \left(\sqrt{\frac{\gamma_{th}}{\bar{\gamma}\mathbb{V}[C]}} + \sqrt{\frac{t^2}{\mathbb{V}[C]}} \right) \right) \qquad (14)$$

Substituting the corresponding values of $\mathbb{V}[C]$, t gives the closed-form expressions to evaluate outage probability.
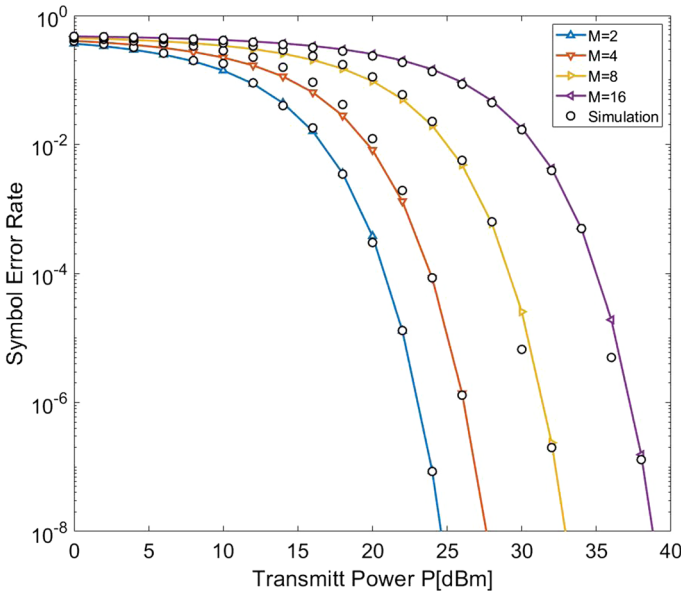
Fig. 5 Symbol error rate of proposed double RIS systems versus P for different modulation order in M-ary PSK $K = 1$, $N = 128$

4 Simulation Results

In this section, we present theoretical and simulation results of SER and outage probability for the single and proposed double RIS system with same number of RIS element in both systems i.e., $N = N_1 + N_2$ to validate the analytical framework. The path-loss at a reference distance of one meter for a carrier frequency of 3 GHz is, $\alpha = (\lambda/4\pi)^2 = -42$ dB and the noise power at destination is set as $\sigma_D^2 = -94$ dBm, and the path loss exponent for all the link is set to 3. The values of P_i, P_c^S and P_c^D are set as 7.8, 10 and 10 milliwatt respectively [12]. The simulation setup for the single RIS and proposed system are shown in Fig. 2. In both systems, source and destination are separated by $d = 100$ metre apart and $h = 5$ meter. In the single RIS, d_1 is fixed at 50 metre and for proposed system, d_1, d_2 are fixed as $d_1 = d_2 = 5$ metre in such a way that $d_{SR_1} d_{R_1D} = d_{SR_2} d_{R_2D}$. The Path loss exponent set $\varrho = 3$ and $\gamma_{th} = 10 dB$ [14] and system operates at a bandwidth (BW) of 10 M Hz.

In Fig. 3, we plot BER of the proposed system under BPSK signalling scheme while varying the parameter N and fixed Rician K factor ($K = 0$) using Eq. (10). Where the solid curves and markers represents the theoretical and simulations respectively. The results unequivocally demonstrate a substantial enhancement in error performance compared to a single RIS system. For example, achieving a target BER of 10^{-6} with a single RIS system demands transmission powers (P) of approximately 47 dBm, 42 dBm, and 36 dBm for corresponding values of N set at 64, 128, and 256. In contrast, in the double RIS system, the same BER of 10^{-6} attainable with lower transmission powers of 35 dBm, 28 dBm, and 22 dBm for N values of 64, 128, and 256, respectively. This observation underscores the superiority of the proposed system in achieving superior BER performance compared
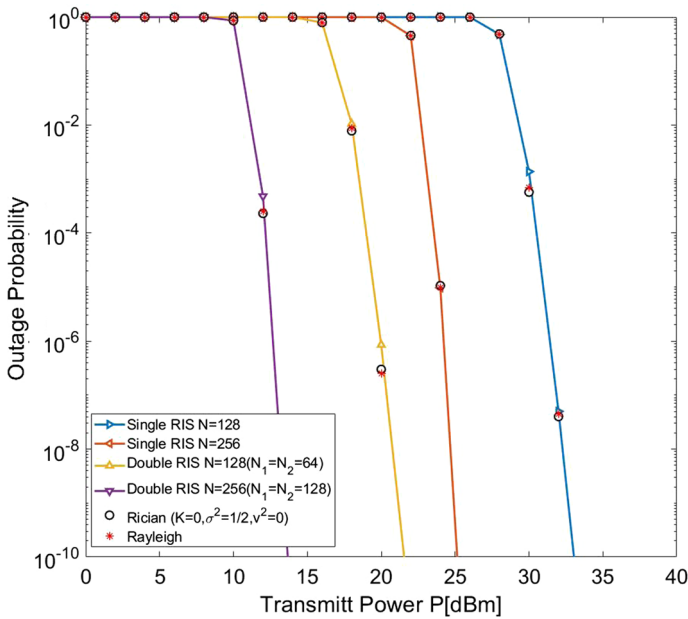
Fig. 6 Outage probability of single RIS and proposed double RIS systems versus P for varying , $K = 0$

Fig. 7 Outage probability of proposed double RIS systems versus P for varying K, $N = 128$
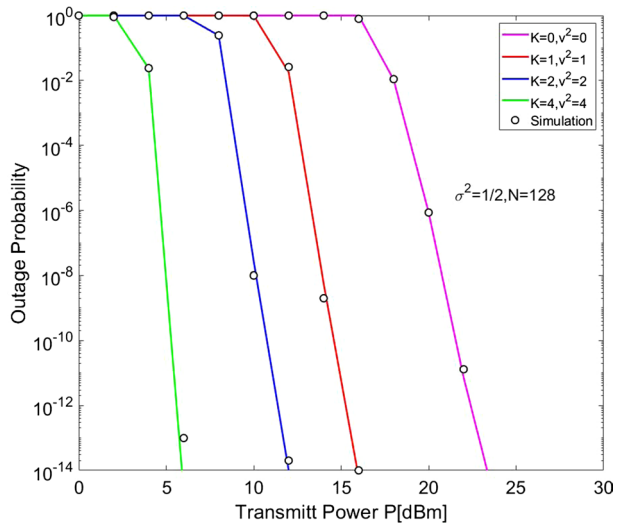
to the base line single RIS system, demanding significantly reduced transmission power. Moreover, the figure also confirms that the special case of Rician channel with $K = 0$ is equivalent to Rayleigh fading scenario.

In Fig. 4, we examine the influence of the Rician K factor on the BER performance of the proposed system. The simulations are performed with a fixed number of reflecting elements, $N = 128$, and $\sigma^2 = 1/2$. As the Rician K factor, representing the power in the LoS

Table 3 Evaluation of G_E

N	System	P^a(dBm) to achieve a BER of 10^{-6}	$E(Joule) = \frac{P+NP_i+P_c^S+P_c^D}{b \times B}$	G_E
64	Single RIS	47	5.063×10^{-6} J	13.7
	Double RIS	35	3.681×10^{-7} J	
128	Single RIS	42	1.686×10^{-6} J	10.2
	Double RIS	28	1.649×10^{-7} J	
256	Single RIS	36	5.997×10^{-7} J	3.59
	Double RIS	22	2.175×10^{-7} J	

^{a}Amount of transmit power is converted to linear scale while calculating the energy consumption gain.

component, increases, the severity of fading diminishes, resulting in an enhancement of BER performance, as visually depicted in Fig. 5. The plotted results illustrate that, for a fixed K value, an incremental increase in the transmitted power corresponds to a gradual reduction in the BER. This observation aligns with the expected behavior, indicating that higher transmit power contributes to improved communication reliability, particularly in scenarios characterized by Rician fading.

Figure 5 illustrates the Symbol Error Rate (SER) of the proposed system as a function of P for different M-ary PSK signaling schemes, incorporating simulations with $N = 128$, $K = 1$ using Eq. (10). The simulations are conducted with. The results demonstrate that, with increasing modulation order (M), the SER performance deteriorates. This behavior aligns with the expectations observed in conventional wireless systems without RIS. In general, higher modulation orders entail a greater sensitivity to channel impairments, leading to increased symbol error rates.

In Fig. 6, we compare the outage probability of both systems with $K = 0$, while varying the parameter N. It can be inferred from Fig. 6 that the theoretical results match with simulation counterparts. As anticipated, in both systems, there is a notable reduction in outage probability for a fixed N as P increases, we observe sharp decrease in outage probability. For example, for $N = 128$, in the single RIS system, the outage probability decreases by a factor of 10 as P transitions from 29 to 31 dBm, and by a factor of 100 as P changes from 32 to 33 dBm. In the proposed system, under the same N, the outage probability decreases by a factor of 10 from 16 to 18 dBm and by a factor of 100 from 20 to 21 dBm. The presented results underscore the efficiency of the proposed system, which exhibits a more pronounced reduction in outage probability for the same changes in transmitted power, particularly in comparison to the single RIS system. Moreover, in Fig. 6, $K = 0$ in a Rician channel mimics Rayleigh fading behaviour.

Figure 7 shows the impact of Rician K factor on the outage probability of proposes system for $N = 128$ and $\sigma^2 = 1/2$. Notably, as we maintain a fixed transmission power P, the outage probability consistently decreases with an escalation in the Rician K factor. This trend suggests that higher K values, indicative of a strong Line-of-Sight (LoS) component, improves the system's resilience against fading conditions.

4.1 Analysis of Energy Consumption Gain (G_E):

Energy consumption gain (G_E), serves as a valuable metric to assert the energy efficiency of the proposed system in comparison to a baseline system. In order to substantiate a claim of enhanced energy efficiency, G_E should exceed one. The definition of G_E, as outlined in reference [25], involves the ratio of energy consumed by the baseline system to achieve a target BER and the energy consumed by the proposed system to achieve the same BER. and expressed as follows:

$$G_E = \frac{E_{singleRIS}}{E_{doubleRIS}}$$

The energy consumed by the system is calculated using the formula, P_{total}/R [26]. In the context of an RIS-aided system, $P_{Total} = P + NP_i + P_c^S + P_c^D$ is the total amount of power consumed by the system to achieve a target BER, where $R = b \times B$ is the rate at which bits are transmitted, b is denoting the bits per symbol (for BPSK, $b = 1$) and B representing the system's bandwidth.

Table 3, clearly highlights the enhanced energy efficiency of the proposed system compared to the single RIS system across all values of N. However, as N increases, there is a noticeable decrease in G_E. This decline is attributed to the concurrent rise in power consumption (NP_i) associated with the increasing number of reflecting elements.

5 Conclusion

In conclusion, this paper introduces and analyses the double RIS-assisted system. By strategically placing the first RIS (R_1) near the source and the second RIS (R_2) near the destination, both independently contribute to communication improvement, especially in scenarios without a direct line between the source and destination. The analysis incorporates moment generating function (MGF)-based symbol error rate (SER) evaluations for Rician and Rayleigh fading channels. A simplified closed-form expression for outage probability (OP) is derived using the Q-function. Through rigorous comparative evaluations, considering an equal number of RIS elements in single and double RIS systems, the proposed approach demonstrates superior performance in terms of SER and OP, all validated through Monte Carlo simulations. Additionally, an in-depth exploration of energy consumption gain reveals that the proposed system outperforms the single RIS system in terms of energy efficiency also.

Declarations

Conflict of interest The authors declare that they have no conflict of interest.

References

1. Basar, E., Di Renzo, M., De Rosny, J., Debbah, M., Alouini, M.-S., & Zhang, R. (2019). Wireless communications through reconfigurable intelligent surfaces. *IEEE Access, 7*, 116753–116773. https://doi.org/10.1109/ACCESS.2019.2935192
2. Wu, Q., & Zhang, R. (2020). Towards smart and reconfigurable environment: intelligent reflecting surface aided wireless network. *IEEE Communications Magazine, 58*(1), 106–112. https://doi.org/10.1109/MCOM.001.1900107
3. Di Renzo, M., et al. (2020). Smart radio environments empowered by reconfigurable intelligent surfaces: How it works, state of research, and the road ahead. *IEEE Journal on Selected Areas in Communications, 38*(11), 2450–2525. https://doi.org/10.1109/JSAC.2020.3007211
4. Wu, Q., Zhang, S., Zheng, B., You, C., & Zhang, R. (2021). Intelligent reflecting surface-aided wireless communications: A tutorial. *IEEE Transactions on Communications, 69*(5), 3313–3351. https://doi.org/10.1109/TCOMM.2021.3051897
5. Boulogeorgos, A.-A.A., & Alexiou, A. (2020). Performance analysis of reconfigurable intelligent surface-assisted wireless systems and comparison with relaying. *IEEE Access, 8*, 94463–94483. https://doi.org/10.1109/ACCESS.2020.2995435
6. Björnson, E., Özdogan, Ö., & Larsson, E. G. (2020). Intelligent reflecting surface versus decode-and-forward: How large surfaces are needed to beat relaying? *IEEE Wireless Communications Letters, 9*(2), 244–248. https://doi.org/10.1109/LWC.2019.2950624
7. You, L., Xiong, J., Ng, D. W. K., Yuen, C., Wang, W., & Gao, X. (2021). Energy efficiency and spectral efficiency tradeoff in ris-aided multiuser mimo uplink transmission. *IEEE Transactions on Signal Processing, 69*, 1407–1421. https://doi.org/10.1109/TSP.2020.3047474
8. Yang, L., Yang, Y., Hasna, M. O., & Alouini, M. S. (2020). Coverage, probability of SNR Gain, and DOR analysis of RiS-aided communication systems. *IEEE Wireless Communications Letters, 9*(8), 1268–1272. https://doi.org/10.1109/LWC.2020.2987798
9. Alanazi, F. (2021). Physical layer security of non orthogonal multiple access using reconfigurable intelligent surfaces. *Wireless Personal Communications*. https://doi.org/10.1007/s11277-021-08985-0
10. Alnwaimi, G., & Boujemaa, H. (2021). Non orthogonal multiple access using reconfigurable intelligent surfaces. *Wireless Personal Communications, 121*(3), 1607–1625. https://doi.org/10.1007/s11277-021-08687-7
11. Alhamad, R., & Boujemaa, H. (2021). Non orthogonal multiple access for millimeter wave communications using intelligent reflecting surfaces. *Wireless Personal Communications*. https://doi.org/10.1007/s11277-021-09021-x
12. Do, T. N., Kaddoum, G., Nguyen, T. L., da Costa, D. B., & Haas, Z. J. (2021). Multi-RIS-aided wireless systems: Statistical characterization and performance analysis. *IEEE Transactions on Communications, 69*(12), 8641–8658. https://doi.org/10.1109/TCOMM.2021.3117599
13. Galappaththige, D. L., Kudathanthirige, D., & Amarasuriya, G. (2020). Performance Analysis of Distributed Intelligent Reflective Surface Aided Communications. In: 2020 IEEE Global Communications Conference, GLOBECOM 2020 - Proceedings, 2020-Janua, 1–30. https://doi.org/10.1109/GLOBECOM42002.2020.9348102
14. Tam, D. T., Nguyen, B. C., Lam, S. C., Vinh, N. V., & Nguyen, T. N. (2023). Ser performance of millimeter-wave communications with multiple reconfigurable intelligent surfaces and transmit antenna selection. *AEU - International Journal of Electronics and Communications, 160*, 154517. https://doi.org/10.1016/j.aeue.2022.154517
15. Yang, L., Yang, Y., Da Costa, D. B., & Trigui, I. (2021). Outage probability and capacity scaling law of multiple RIS-aided networks. *IEEE Wireless Communications Letters, 10*(2), 256–260. https://doi.org/10.1109/LWC.2020.3026712
16. Li, J., Zhang, L., Xue, K., Fang, Y., & Sun, Q. (2021). Secure transmission by leveraging multiple intelligent reflecting surfaces in MISO systems. *IEEE Transactions on Mobile Computing, 1233*, 1–14. https://doi.org/10.1109/TMC.2021.3114167
17. Yang, Z., et al. (2022). Energy-efficient wireless communications with distributed reconfigurable intelligent surfaces. *IEEE Trans- actions on Wireless Communications, 21*(1), 665–679. https://doi.org/10.1109/TWC.2021.3098632
18. Yang, S., Lyu, W., Xiu, Y., Zhang, Z., & Yuen, C. (2023). Active 3D double-ris-aided multi-user communications: Two-timescale-based separate channel estimation via bayesian learning. *IEEE Transactions on Communications, 71*(6), 3605–3620. https://doi.org/10.1109/TCOMM.2023.3265115

19. Han, Y., Zhang, S., Duan, L., & Zhang, R. (2020). Cooperative double-IRS aided communication: Beamforming design and power scaling. *IEEE Wireless Communications Letters, 9*(8), 1206–1210. https://doi.org/10.1109/LWC.2020.2986290

20. Dong, L., Wang, H. M., Bai, J., & Xiao, H. (2021). Double Intelligent Reflecting Surface for Secure Transmission with Inter-Surface Signal Reflection. *IEEE Transactions on Vehicular Technology, 70*(3), 2912–2916. https://doi.org/10.1109/TVT.2021.3062059

21. Proakis, J. G. (2008). Digital communications (5th ed.). McGraw- Hill.

22. Simon, M., & Alouini, M. S. (2005). *Digital communications over fading channels* (2nd ed.). Wiley.

23. Sun, Y., Baricz, Á., & Zhou, S. (2010). On the monotonicity, log-concavity, and tight bounds of the generalized marcum and nuttall Q-functions. *IEEE Transactions on Information Theory, 56*(3), 1166–1186. https://doi.org/10.1109/TIT.2009.2039048

24. Gradshteyn, I. S., & Ryzhik, I. M. (2007). *Table of integrals, series, and products* (7th ed.). Academic.

25. Han, C., et al. (2011). Green radio: Radio techniques to enable energy-efficient wireless networks. *IEEE Communications Magazine, 49*(6), 46–54. https://doi.org/10.1109/MCOM.2011.5783984

26. Zhang, J., Fei, L., Gao, Q., & Peng, X.-H. (2011). Energy-efficient multihop cooperative MISO transmission with optimal HopdistanceinwirelessAdHoc networks. *IEEE Transactions on Wireless Communications, 10*(10), 3426–3435. https://doi.org/10.1109/TWC.2011.081011.102210

27. Annamalai A, Tellambura C, Matyjas J. A new twist on the generalized Marcum Q-function QM (a, b) with fractional-order M and its applications. In2009 6th IEEE consumer communications and networking conference 2009 Jan 10 (pp. 1-5). IEEE.

Publisher's Note Springer Nature remains neutral with regard to jurisdictional claims in published maps and institutional affiliations.

R. Mahammad Rafi received his B.Tech degree in Electronics and Communication Engineering from Jawaharlal Nehru Technological University, Anantapur, India in 2013 and the M.Tech degree in Communications and Signal Processing from Jawaharlal Nehru Technological University, Anantapur, India in 2016. He is currently working towards his Ph.D. degree in National Institute of Technology (NIT), Tiruchirappalli, Tamilnadu, India from 2019. His research interests include mmwave communication, reconfigurable intelligent surface, and channel modeling.

Sudha Vaiyamalai received her B.E degree in Electronics and Communication Engineering from Bharathidasan University, India in 2000 and the M.E degree in Communication Systems from Anna University, India in 2006. She has completed her Ph.D. in the area of wireless communication systems at National Institute of Technology, Tiruchirappalli in 2017. She has 22 years of teaching experience. Currently, she is working as Associate Professor in the Department of Electronics and Communication Engineering, National Institute of Technology (NIT), Tiruchirappalli, India. Her research interests include Multicarrier Wireless Systems, Digital Communication, Wireless Optical Communication, Wireless Networks. She has published several papers in International Journals and Conferences. She is a life member of ISTE